Hydrol. Earth Syst. Sci. Discuss., 7, 2053–2084, 2010
www.hydrol-earth-syst-sci-discuss.net/7/2053/2010/

Hydrology and Earth System Sciences Discussions

This discussion paper is/has been under review for the journal Hydrology and Earth System Sciences (HESS). Please refer to the corresponding final paper in HESS if available.

Possibilistic uncertainty analysis of a conceptual model of snowmelt runoff

A. P. Jacquin

Facultad de Ingeniería, Pontificia Universidad Católica de Valparaíso, Av. Brasil 2147, Valparaíso, Chile

Received: 11 March 2010 – Accepted: 15 March 2010 – Published: 24 March 2010

Correspondence to: A. P. Jacquin (alexandra.jacquin@ucv.cl)

Published by Copernicus Publications on behalf of the European Geosciences Union.

Abstract

This study presents the analysis of predictive uncertainty of a conceptual type snowmelt runoff model. The method applied uses possibilistic rather than probabilistic calculus for the evaluation of predictive uncertainty. Possibility theory is an information theory meant to model uncertainties caused by imprecise or incomplete knowledge about a real system rather than by randomness. A snow dominated catchment in the Chilean Andes is used as case study. Predictive uncertainty arising from parameter uncertainties of the watershed model is assessed. Model performance is evaluated according to several criteria, in order to define the possibility distribution of the model representations. The likelihood of the simulated glacier mass balance and snow cover are used for further assessing model credibility. Possibility distributions of the discharge estimates and prediction uncertainty bounds are subsequently derived. The results of the study indicate that the use of additional information allows a reduction of predictive uncertainty. In particular, the assessment of the simulated glacier mass balance and snow cover helps to reduce the width of the uncertainty bounds without a significant increment in the number of unbounded observations.

1 Introduction

Uncertainty can be defined as the lack of necessary information to "quantitatively and qualitatively... describe, prescribe, or predict deterministically and numerically a system, its behaviour or other characteristica" (Zimmermann, 2001). Even the most complex model of a real system necessarily involves a series of assumptions and approximations, which are necessary to compensate for our incomplete understanding of the real world. Unfortunately, the question of whether or not these assumptions and approximations are justifiable can hardly be answered with absolute certitude, which implies that the reliability of the model is ultimately uncertain. Watershed models, in particular, attempt to simulate the complex and interacting hydrological processes that lead to the transformation of precipitation into runoff. The sources contributing to the overall uncertainty in the discharge estimates provided by these models can be grouped in three categories, namely, data uncertainty, model structure uncertainty and parameter uncertainty (Bates and Townley, 1988; Lei and Shilling, 1996).

It is widely recognized that because of these uncertainties and their implications, choosing a single model representation (i.e. a combination of a model structure and a parameter set) for simulating runoff generation in a particular catchment is a common practice that is not necessarily supported by evidence (see e.g. Beven, 2006; Wagener et al., 2003). Most likely, there may be many acceptable model representations whose rejection cannot be justified, considering the always limited information available to the modeller. This non-uniqueness of the model representations, sometimes called equifinality in the hydrological literature (Beven and Freer, 2001; Beven, 2006), is a problem that has long been recognized in the context of linear systems theory (see e.g. Cheng, 1959; Zadeh and Desoer, 1963). Nevertheless, reality outside the scientific context is that field practitioners rarely include an analysis of predictive uncertainty when applying watershed models in water resources studies. Moreover, as explained by Pappenberger and Beven (2006), there is an important number of water researchers still unconvinced that uncertainty analysis should necessarily be part of the modelling process.

In spite of the reluctance of some scientists, hydrologists have been very active in developing methods for analyzing predictive uncertainty (see e.g. Matott et al., 2009; Montanari et al., 2009). Probabilistic approaches include variance propagation (e.g. Kuczera, 1988; Bates and Townley, 1988), Monte Carlo sampling coupled with frequency analysis (e.g. Bates and Townley, 1988; Yu et al., 2001; Thorsen et al., 2001; Zehe and Blöschl, 2004; Arnold et al., 2009) and Bayesian analysis (e.g. Beven and Binley, 1992; Romanowicz et al., 1994; Thiemann et al., 2001; Misirli et al., 2003; Engeland et al., 2005; Rojas et al., 2010; Renard et al., 2010). Non-probabilistic methods found in the literature include those based on fuzzy sets theory and possibility theory (e.g. Dou et al., 1997; Seibert, 1997; Freissinet et al., 1999; Özelkan and Duckstein, 2001; Bárdossy et al., 2006; Jacquin and Shamseldin, 2007; Zhang et al., 2009). Non-probabilistic frameworks or subjective probability approaches are a suitable alternative for analysing model structure and parameter uncertainties, which have an epistemic rather than a stochastic nature. Furthermore, these methods may be the only available in situations of data scarcity, where subjective expert knowledge has to be incorporated as an additional source of information (Montanari et al., 2009).

In this study, predictive uncertainty of a conceptual type snowmelt runoff model is analysed using the method proposed by Jacquin and Shamdeldin (2007). This method, based on possibility theory (Zadeh, 1978, 1981), explicitly accounts for the problem of the non-uniqueness of model representations. So far, the method has been tested in very few cases, all of which correspond to models without a snowmelt runoff component (Jacquin and Shamdeldin, 2007, 2009). The applicability of the method to other model structures has not been explored. Furthermore, the effect of several subjective choices made during the inference process, such as the possibility level at which uncertainty bounds are derived and the criteria used for the evaluation of model credibility, have not been analysed.

2 Possibilistic method for uncertainty analysis

In recent years, Jacquin and Shamseldin (2007) proposed an uncertainty analysis method that was originally inspired by the widely known Generalized Likelihood Uncertainty Estimation (GLUE) methodology (Beven and Binley, 1992). The difference between both methods is that GLUE follows a subjective probabilistic scheme, but the method analysed herein uses possibilistic calculus in order to assess predictive uncertainty. More concretely, the derivation of uncertainty bounds within the GLUE methodology relies on the calculation of prediction quantiles from the likelihood weights of the model predictions at each time step, while the possibilistic method applies the Extension Principle (Zadeh, 1981) in order to obtain the possibility distribution of the discharge predictions. The possibility of a discharge prediction is a value $0 \leq \alpha \leq 1$ that is indication of its credibility, where the most credible model representations achieve a possibility equal to unity and unfeasible model realizations are assigned a possibility equal to zero. At each time step, the α possibility bounds enclose all the discharge predictions having possibility values strictly higher than α. The α possibility bounds should not be interpreted in a frequentist sense, because there is no reason to expect that the uncertainty bounds at any given possibility level α enclose a fixed fraction α of the observations.

Possibility theory is an information theory of partial belief that focuses on epistemic uncertainties. Accordingly, the method analysed herein is based on the premise that the adequacy of a watershed model to describe the catchment's response is uncertain because the knowledge available to the modeller is limited and not because of randomness. These uncertainties have a subjective nature, in the sense that they are related with the information available to the observer and they could be reduced by improving it (Ferson and Ginzburg, 1996). Even though subjective probabilities can also be used for describing degrees of belief (e.g. the GLUE methodology), possibility and probability theories are complementary rather than competitive, because they are meant to describe different levels of information (Klir and Folger, 1992; Dubois and Prade, 1993; Ross et al., 2002). A discussion on the advantages of a possibilistic framework with respect to probabilities for uncertainty analysis of watershed models can be found in the work by Jacquin and Shamseldin (2007).

Similar to the GLUE methodology, the possibilistic method also allows the estimation of predictive uncertainty arising from model structure and parameter uncertainties using Monte Carlo simulations. However, the following discussion assumes that a single model structure is being considered and that only parameter uncertainty is being analysed. In this case, the Monte Carlo sample of model realizations is obtained by generating a large sample of the parameter vector $\boldsymbol{\theta}$. The prior possibility distribution of the model realizations, π_{prior}, is subsequently derived from the available prior knowledge about the regions of the parameter vector $\boldsymbol{\theta}$ associated with good model realizations.

The goodness of fit of the model realizations is further evaluated using a chosen performance measure, together with a model rejection criterion. The values of this performance measure are used for deriving the possibility distribution of the model realizations, π, where model realizations achieving possibility values $\pi(\boldsymbol{\theta})$ equal to one are seen as the most credible and those having possibilities values equal to zero are considered unrealistic. The information provided by the possibility distribution π allows updating the prior possibility distribution, obtaining the posterior possibility distribution of the model representations, given by

$$\pi_{\text{post}}(\boldsymbol{\theta}) = \frac{\pi_{\text{prior}}(\boldsymbol{\theta}) \cdot \pi(\boldsymbol{\theta})}{\max\limits_{\theta} \left\{ \pi_{\text{prior}}(\boldsymbol{\theta}) \cdot \pi(\boldsymbol{\theta}) \right\}}. \tag{1}$$

In the case where more than one performance criteria is considered, the posterior possibility distribution is repeatedly updated through application of Eq. (1). The use of additional performance criteria is expected to provide new knowledge about the goodness of the model realizations, thus reducing predictive uncertainty.

The possibility distribution of the discharge predictions at each time step t is finally obtained from the posterior possibilities $\pi_{\text{post}}(\boldsymbol{\theta})$. Given a particular model structure and input data, the model output Q_t^* at time t is a deterministic function of the model parameters $\boldsymbol{\theta}$. By virtue of the Extension Principle (Zadeh, 1981), the possibilites of the discharge estimates Q_t^* are given by

$$\pi_{\text{post}}^{(t)}(q^*) \begin{cases} \max\limits_{Q_t^*(\boldsymbol{\theta})=q^*} \pi_{\text{post}}(\boldsymbol{\theta}) \\ 0, \quad \text{if} \quad Q_t^*(\boldsymbol{\theta}) \neq q^* \quad \text{for all } \boldsymbol{\theta} \end{cases}, \tag{2}$$

where q^* is a possible value of Q_t^*. Equation (2) implies that model realizations with possibility values $\pi_{\text{post}}(\boldsymbol{\theta})$ equal to zero are implicitly discarded from the sample, because only simulations with possibility values $\pi_{\text{post}}(\boldsymbol{\theta})$ strictly greater than zero effectively contribute in the derivation of the uncertainty bounds. The upper and lower bounds of the strong α-cuts of the possibility distribution $\pi_{\text{post}}^{(t)}$, i.e. the set of all values

HESSD

7, 2053–2084, 2010

Uncertainty analysis of a conceptual model of snowmelt runoff

A. P. Jacquin

q^* with possibility values $\pi^{(t)}_{\text{post}}(q^*)$ strictly greater than α, define the α possibility bounds of the discharge predictions. If the possibility distribution $\pi^{(t)}_{\text{post}}$ is convex, the α possibility bounds define intervals of discharge predictions with at least a possibility α of being a good approximation to the observations. Otherwise, this interpretation is only valid for α values that are higher than all local maxima different from the global maximum, and for α values that are lower than all local minima of $\pi^{(t)}_{\text{post}}$.

3 Model description

The model analyzed is a conceptual type snowmelt runoff model that is widely used in water resources studies for the mining industry in Chile (e.g. Water Management Ltda., 2001; Arcadis Geotécnica, 2007). The version of the model used here is due to Kamann (1998) and it operates at a monthly time step. The hydrometeorological information required includes precipitation, number of rain days, evaporation, temperature, air humidity, wind speed and cloud cover. The model output is given by the monthly discharge at the catchment's outlet. In the manner computationally implemented in this study, the model has a total of 16 independent parameters.

The model divides the catchment into five elevation zones, where the fifth zone corresponds to the catchment glaciers. Snowmelt is calculated using an energy balance method, where incident solar radiation is estimated with an empirical formula locally adjusted for the Andes Mountains of Central Chile (Espíldora, 1968) and albedo values are obtained from the empirical curves of Amorocho and Espíldora (1966). In the case of the fifth elevation zone, glaciers are seen as an inexhaustible source of water that melts when the snow cover is depleted. An individual surface-soil moisture balance is performed within each elevation zone, in order to generate its contribution to direct runoff and groundwater recharge. With the aim of simulating the diffusion and attenuation effects of the catchment, routing elements are incorporated to the model. Direct runoff components from the individual elevation zones are routed through separate

HESSD
7, 2053–2084, 2010

linear reservoirs; the catchment's total direct runoff is finally obtained by sumation of the routed direct runoff contributions from the individual elevation zones. Groundwater recharge at the catchment level is calculated as the sum of groundwater recharge from the individual elevation zones and further routed through a single linear reservoir, in order to obtain the total generated groundwater runoff. Total estimated discharge corresponds to the sum of total surface and total groundwater runoff.

4 Catchment and data

The study area is located in the Andean region of Central Chile. Maipo River at El Manzano is a snow dominated catchment with a surface of 4968 Km^2, where approximately 8% was covered by glaciers at the time when the data used in this study were collected (Valdivia, 1984). Elevation ranges from 890 m a.s.l. to 6570 m a.s.l., with a median altitude of 3200 m a.s.l. Glacier areas are located above 3500 m a.s.l. (Valdivia, 1984).

Precipitation is mostly produced by cold fronts that arrive in the area during winter. Accordingly, as shown in Fig. 1, most precipitation occurs between May and August, while precipitation amounts during the rest of the year are relatively low. The observed snowline in the area is located about 2100 m a.s.l. during May–September, which implies that most precipitation corresponds to snowfall. Except for snow and glacier zones in the higher areas, snow cover in the catchment is lost by the end of the melting period. As seen in Fig. 1, monthly mean discharge is minimal in May–August, but it increments during the melting season September–March; monthly discharge reaches its maximum value in December or January. Human intervention in the catchment's hydrological regime at the time when the data used in this study were collected was not significant. Glacier mass balance studies in the area are scarce. However, it has been estimated that, in average, glaciers in Central Chile experienced a mass loss Δh_{med}=0.45–0.95 m/year of equivalent water depth in the period 1945–1996 (Rivera et al., 2002). This mass loss does not occur in a systematic manner, as negative mass balances alternate with positive mass balances in El Niño years.

In this study, the hydrological year is defined from 1 May (coinciding with the minimum monthly mean discharge and also the beginning of heavy precipitation) to 30 April. Data available for the study consists of monthly time series during the hydrological years 1962/63–1990/92. The available data were divided into a calibration period (1962/63–1982/83) and a verification period (1983/84–1990/91) for split sampling tests. The first year of calibration is used as a warming-up period.

5 Methodology

5.1 Monte Carlo sampling and prior possibilities

A Monte Carlo sample of the parameter vector is generated using the uniform random number generator, by varying all 16 parameters simultaneously. The chosen sample size is 80 000, as preliminary experiments revealed that further increases in the number of parameter vectors did not have a significant impact in the prediction uncertainty bounds. The feasible ranges for the model parameters are defined so that they are wider than the ranges of optimal parameter values found in previous applications of the model.

Prior possibilities of model realizations are defined according to

$$\pi_{\text{prior}}(\boldsymbol{\theta}) = \begin{cases} 1, \text{if } \boldsymbol{\theta} \in \Omega \\ 0, \text{otherwise} \end{cases}, \tag{3}$$

where Ω is the feasible space of the parameter vector. Equation (3) implies that the prior possibility values $\pi_{\text{prior}}(\boldsymbol{\theta})$ of all the model realizations in the sample, whose parameters are necessarily inside the corresponding feasible ranges, are assigned a prior possibility of unity.

5.2 Evaluation of model performance

The possibility distributions of the model representations are subsequently obtained through evaluation of the goodness of fit of the estimated discharge hydrographs. Model performance is first evaluated according to the mean squared error of the Box-Cox transformed discharge ($\mathrm{MSE_{BC}}$), as seen in previous studies (Thiemann et al., 2001; Misirli et al., 2003), which reduces the effect of heteroscedasticity and emphasizes the importance of the model performance during low flow periods. The associated possibility distribution is defined by

$$\pi_1(\boldsymbol{\theta}) = \begin{cases} \frac{V_{\mathrm{BC}} - \mathrm{MSE_{BC}}}{V_{\mathrm{BC}} - \min\{\mathrm{MSE_{BC}}\}}, \mathrm{MSE_{BC}} \leq V_{\mathrm{BC}} \\ 0, \text{otherwise} \end{cases} \tag{4}$$

where V_{BC} is the variance of the Box-Cox transformed observed discharge during the calibration period, and $\min\{\mathrm{MSE_{BC}}\}$ represents the lowest $\mathrm{MSE_{BC}}$ value found among all the model realizations in the sample. The chosen model rejection criterion specifies that model realizations with $\mathrm{MSE_{BC}}$ values greater than V_{BC} are assigned a possibility $\pi_1(\boldsymbol{\theta})$ equal to zero. The choice of this behavioural threshold is based on the interpretation that $\mathrm{MSE_{BC}}$ values greater than V_{BC} indicate that the model is outperformed by a naïve model whose Box-Cox transformed output is always equal to the mean Box-Cox transformed observed discharge during the calibration period.

The second possibility distribution used for constraining the model representations is based on the volumetric errors, as in the work by Jacquin and Shamseldin (2007). This possibility distribution is defined as

$$\pi_2(\boldsymbol{\theta}) = \begin{cases} \frac{1 - |\mathrm{REVF}|}{1 - \min\{|\mathrm{REVF}|\}}, 0 \leq |\mathrm{REVF}| \leq 1 \\ 0, \text{ otherwise} \end{cases}, \tag{5}$$

where |REVF| represents the absolute value of the relative error of the volumetric fit of the model representation during the calibration period, given by

$$\mathrm{REVF}=1-\frac{\sum Q_t^*}{\sum Q_t}, \quad (6)$$

and min{|REVF|} corresponds to the smallest |REVF| value in the sample The model rejection criterion implicit in Eq. (5) consists in the removal of the model realizations with absolute volumetric errors greater than 100% during the calibration period.

The last possibility distribution used in this study is intended to asses the ability of the models to estimate the discharge peaks. The value of the possibility distribution is calculated according to

$$\pi_3(\boldsymbol{\theta})=\begin{cases}\frac{1-\mathrm{REP}}{1-\min\{\mathrm{REP}\}}, 0\leq \mathrm{REP}\leq 1\\ 0,\ \text{otherwise}\end{cases}, \quad (7)$$

where the quantity REP represente the average relative error to the peak. This is given by

$$\mathrm{REP}=\sum_{i=1}^{N_\mathrm{p}}\frac{|Qp_t-Qp_t^*|}{N_\mathrm{p}Qp_t}, \quad (8)$$

where N_p is the number of selected flow peaks, Qp_t represents a peak in the observed hydrograph, and Qp_t^* is the model estimated discharge for the same time step as Qp_t. The quantity min{REP} in Eq. (7) is the smallest REP value among all the model realizations in the sample. The model rejection criterion specified by Eq. (7) is the removal of the realizations whose REP values are greater than 100% during the calibration period.

The normalization factors $V_\mathrm{BC}-\min\{\mathrm{MSE}_\mathrm{BC}\}$, $1-\min\{|\mathrm{REVF}|\}$ and $1-\min\{\mathrm{REP}\}$ in Eq. (4), (5) and (7), respectively, are introduced in order to obtain possibility values with a maximum empirical value of unity. The rationale of this choice is that the simulation providing the most credible representation of the real system, as indicated by the measure of model performance used in each case, is assigned a possibility equal to unity. Model rejection criteria more restrictive than those specified by Eq. (4), (5) and (7) are not considered necessary within the possibilistic framework, as model realizations with low possibility values do not affect the α-cuts associated with high possibilities.

5.3 Posterior possibility distributions of the model realizations

Once the possibility values $\pi_{\text{prior}}(\boldsymbol{\theta})$, $\pi_1(\boldsymbol{\theta})$, $\pi_2(\boldsymbol{\theta})$ and $\pi_3(\boldsymbol{\theta})$ have been obtained, the posterior possibilities of the simulations are derived using the combination rule of Eq. (1). The first posterior possibility distribution defined uses only the information provided by the mean squared error of the Box-Cox transformed discharge for constraining the model representation. Accordingly, the posterior possibilities $\pi_{\text{post\_1}}(\boldsymbol{\theta})$ are obtained after substitution of $\pi(\boldsymbol{\theta})$ by $\pi_1(\boldsymbol{\theta})$ in Eq. (1). The posterior possibilities $\pi_{\text{post\_1}}(\boldsymbol{\theta})$ are subsequently updated by incorporation of the information on the volumetric fit of the models. The possibility distribution π_2 and the possibility distribution $\pi_{\text{post\_1}}$ are thus combined according to Eq. (1), in order to obtain the updated posterior possibility distribution $\pi_{\text{post\_1,2}}$. Similarly, the information on the ability of the models to estimate the discharge peaks is used to further constrain the model representations. The possibility distribution π_3 and the possibility distribution $\pi_{\text{post\_1,2}}$ are combined according to Eq. (1), obtaining the updated possibility distribution $\pi_{\text{post\_1,2,3}}$.

5.4 Derivation of prediction uncertainty bounds

As explained in Sect. 2, the possibility distribution of the discharge predictions is obtained from the information provided by the posterior possibilities of the model realizations. The posterior possibility distributions $\pi_{\text{post\_1}}$, $\pi_{\text{post\_1,2}}$ and $\pi_{\text{post\_1,2,3}}$ are substituted in Eq. (2) for deriving the possibility distributions $\pi^{(t)}_{\text{post\_1}}$, $\pi^{(t)}_{\text{post\_1,2}}$ and $\pi^{(t)}_{\text{post\_1,2,3}}$, respectively. Possibility bounds of these possibility distributions are finally derived at several possibility levels α, in order to evaluate the effect of the possibility level on the characteristics of the uncertainty bounds.

5.5 Alternative definition of the prior possibility distribution

An alternative definition of the prior possibilities of the model realizations is also tested. This prior possibility distribution, which evaluates the likelihood of the simulated glacier mass balance and snow cover at the end of the calibration period, is given by

$$\pi_0(\boldsymbol{\theta}) = \begin{cases} 1, \text{if } (\boldsymbol{\theta} \in \Omega) \text{ and } (\text{glacbal} > -2\,\text{m/year} \cdot N_{\text{cal}}) \text{ and } (\text{snowac} = 0) \\ 0, \text{otherwise} \end{cases}, \tag{9}$$

The variable "glacbal" in Eq. (9) represents the accumulated surface mass balance between precipitation, evapotranspiration and melt in the glacier zone, from the end of the warming-up period until the end of the calibration period. N_{cal} is the number of years of the calibration period. Accumulated glacier mass losses exceeding 2 times the average values reported in the literature for the study area (see Sect. 4) are considered unrealistic and prior possibilities for these model realizations are set to zero. The variable "snowac" in Eq. (9) represents the snow water equivalent accumulated in the elevations zones below the 2 °C isothermal line by the end of the calibration period, which should be null according to what was discussed in Sect. 4. Model realizations yielding snow accumulations that do not fulfill this requirement are assigned a prior possibility $\pi_0(\boldsymbol{\theta})$=0.

In analogy to what was described in Sect. 5.3, posterior possibility distributions of the model representations are derived using $\pi_0(\boldsymbol{\theta})$ as prior possibility distribution instead of $\pi_{\text{prior}}(\boldsymbol{\theta})$. The posterior possibility distributions obtained are denoted $\pi_{\text{post\_0,1}}$, $\pi_{\text{post\_0,1,2}}$ and $\pi_{\text{post\_0,1,2,3}}$. Finally, these posterior possibility distributions are used for deriving possibility distributions of the discharge predictions, named $\pi^{(t)}_{\text{post\_0,1}}$,$\pi^{(t)}_{\text{post\_0,1,2}}$ and $\pi^{(t)}_{\text{post\_0,1,2,3}}$, respectively, and prediction uncertainty bounds.

6 Results

6.1 Number of simulations retained according to different criteria

Firstly, it was observed that the effective sample size notably reduces when π_0, defined by Eq. (9), is used as a prior possibility distribution. In particular, only 28 859 simulations among 80 000 in the Monte Carlo sample obtained prior possibilities $\pi_0(\boldsymbol{\theta})>0$. This situation is mainly due to the restriction imposed to the simulated snow cover, which was only fulfilled by 28 902 model realizations; by contrast, the restriction imposed to the mass balance in the glaciers was achieved by most of the simulations (75 043).

Figure 2 shows the total number of simulations retained above different possibility levels α of the possibility distributions π_{post_1}, $\pi_{post\_1,2}$ and $\pi_{post\_1,2,3}$. Similarly, Fig. 3 shows the total number of simulations retained above different possibility levels α of the possibility distributions $\pi_{post\_0,1}$, $\pi_{post\_0,1,2}$ and $\pi_{post\_0,1,2,3}$. These plots reveal that the rejection criterion specified by possibility distribution π_1 is quite restrictive; the number of simulations having posterior possibilities $\pi_{post\_1}(\boldsymbol{\theta})$ and $\pi_{post\_0,1}(\boldsymbol{\theta})$ greater than zero is about 40% the number of simulations with nonzero prior possibilities $\pi_{prior}(\boldsymbol{\theta})$ and $\pi_0(\boldsymbol{\theta})$, respectively. Figures 2 and 3 also demonstrate that the total number of simulations retained above a given possibility level α decreases as more information is used for defining the posterior possibility distribution of the model representations. The most notable reductions are generally seen when the information on the peak errors is used for updating the posterior possibilities of the simulations, (i.e. when using $\pi_{post\_1,2,3}$ instead of $\pi_{post\_1,2}$).

6.2 Performance of the simulations retained according to different criteria

Figure 4 shows ranges of model efficiency R^2 (Nash and Sutcliffe, 1970), REVF and REP values obtained during the verification period by the simulations retained above different possibility levels α of the possibility distributions π_{post_1}, $\pi_{post\_1,2}$ and

HESSD
7, 2053–2084, 2010

$\pi_{post\_1,2,3}$. Figure 5 shows analogous information for the case of the possibility distributions $\pi_{post\_0,1}$, $\pi_{post\_0,1,2}$ and $\pi_{post\_0,1,2,3}$.

Figure 4 demonstrates that R^2, |REVF| and REP values of some of the simulations retained about the possibility level 0% are quite poor (i.e. low R^2 values, high |REVF| and high REP values). Including more information in the model selection criterion does not help to remove these underperforming simulations, unless the possibility level α is increased. At possibility levels $\alpha > 0$, the lower bound of the efficiency values R^2 observed during the verification period can normally be raised by moving from the possibility distribution π_{post_1} to $\pi_{post\_1,2}$; a further increase in this lower bound is normally achieved if $\pi_{post\_1,2,3}$ is used instead of $\pi_{post\_1,2}$. It can also be observed that, at possibility levels $\alpha > 0$, replacing the possibility distribution π_{post_1} by $\pi_{post\_1,2}$ usually produces a significant decrease in the highest |REVF| and REP values observed during the verification period. In general, a further improvement in |REVF| and REP values is generally observed if $\pi_{posterior\_1,2,3}$ is used instead of $\pi_{posterior\_1,2}$.

The situation shown in Fig. 5 for the case of the possibility distributions $\pi_{post\_0,1}$, $\pi_{post\_0,1,2}$ and $\pi_{post\_0,1,2,3}$ is similar to that of Fig. 4. Including more information in the definition of the possibility distribution of the model realizations does not help to remove underperforming simulations at the possibility level 0%; but, model performance of the simulations retained above possibility levels $\alpha > 0$ generally improves when moving from $\pi_{post\_0,1}$ to $\pi_{post\_0,1,2}$, and from $\pi_{post\_0,1,2}$ to $\pi_{post\_0,1,2,3}$. Comparison of Figs. 4 and 5 further reveals that using the prior possibility distribution π_0 instead of π_{prior} results in an improvement in the performance of the simulations retained at low-medium possibility levels, although this positive feature is not so evident at high possibility levels.

6.3 Possibility bounds of the discharge estimates

Figure 6 shows selected possibility bounds (0%, 75% and 90%) for the hydrological year 1983/84; this figure corresponds to the case where the posterior possibilities of the simulations are given by $\pi_{post\_1}(\boldsymbol{\theta})$. The concurrent time series of rainfall amounts and observed discharges are also shown. The 0% possibility bounds are obtained by including the discharge estimations of all the behavioural simulations. Figure 7 shows possibility bounds for the hydrological year 1983/84, derived from the posterior possibilities $\pi_{\text{post\_1,2,3}}(\boldsymbol{\theta})$.

Not surprisingly, Figs. 6 and 7 demonstrate that increasing the possibility level α reduces the width of the prediction intervals within the possibility bounds. More interestingly, it can be observed that uncertainty in the predictions of the model is generally large with respect to the magnitude of the concurrent discharge observations. Moreover, the distance between the uncertainty bounds tends to increase with the magnitude of the observed discharge, which indicates an increase in predictive uncertainty. However, incorporating more information in the calculation of the posterior possibilities of the model representations generally has a narrowing effect in the possibility bounds, which reduces predictive uncertainty. For example, Fig. 8 shows the prediction width for the posterior possibility distributions $\pi_{\text{post\_1}}$, $\pi_{\text{post\_1,2}}$ and $\pi_{\text{post\_1,2,3}}$. Similarly, a reduction of prediction width generally occurs if the definition of the priors changes from $\pi_{\text{prior}}(\boldsymbol{\theta})$ to $\pi_0(\boldsymbol{\theta})$, as seen in Fig. 9.

As in the study by Montanari (2005), the performance of the uncertainty bounds is assessed in terms of their ability to enclose the discharge observations. Table 1 shows the fraction of the observations outside selected possibility bounds (0%, 75% and 90%) of different posterior possibility distributions, during the verification period. As discussed above, incorporating more information in the calculation of the posterior possibilities of the simulations has a narrowing effect in the width of the possibility bounds. As a result, the number of observations not bracketed by the possibility bounds generally increases. This situation is also observed when comparing the fraction of outliers obtained with the prior possibilities $\pi_0(\boldsymbol{\theta})$ and that obtained with the priors $\pi_{\text{prior}}(\boldsymbol{\theta})$, which are generally slightly lower. As seen in Table 1, the 50% and 75% possibility bounds enclose the majority of the observations. Table 1 also reveals that the effect of further increasing the possibility level to 90% is that the possibility bounds fail to enclose a larger fraction of the observations, although this situation is still unfrequent.

HESSD
7, 2053–2084, 2010

Uncertainty analysis of a conceptual model of snowmelt runoff

A. P. Jacquin

7 Conclusions

This study has presented the application of the method proposed by Jacquin and Shanseldin (2007) to the analysis of predictive uncertainty of a conceptual type snowmelt runoff model. This method uses possibilistic rather than probabilistic calculus for the evaluation of predictive uncertainty in watershed modelling. A snow dominated catchment in the Chilean Andes is used as case study. Predictive uncertainty arising from parameter uncertainties of the watershed model is assessed using the possibilistic method. The main conclusions of the study are summarized as follows.

It was observed that the number of behavioral simulations (i.e. the model realizations with possibility values α strictly greater than zero) was relatively low compared to the total sample size. This result is in agreement with previous applications of the method (Jacquin and Shamseldin, 2007, 2009). In the case of this study, this situation is mainly due to the severity of the rejection criterion implicit in possibility distribution π_1, based on the mean squared error of the Box-Cox transformed discharge, as seen in Eq. (4). The use of the alternative prior possibility distribution π_0, which evaluates the credibility of the simulated glacier mass balance and snow cover according to Eq. (9), notably reduces the sample size of behavioural simulations. In spite of this filtering process, it was found that the performance of some of the model realizations retained above the posibility level $\alpha = 0$ was poor, and that using additional model performance criteria did not help removing these unperforming simulations. At possibility levels $\alpha > 0$, however, the performance of the simulations retained tends to improve as more information is used for constraining the model simulations. In particular, using the prior possibility distribution π_0 instead of π_{prior} helps to remove the worst simulations retained at low and medium possibility levels.

In additon to this, it was seen that predictive uncertainty of the model was relatively large with respect to the magnitude of the concurrent discharge observations, but using additional information for constraining the model representations allowed reducing it. In particular, a reduction of prediction width is generally achieved if the definition

HESSD
7, 2053–2084, 2010

of the priors assesses the simulated snow cover and glacier mass balance (i.e. if the possibility distribution π_0 is used), without a significant increase in the number of observations not enclosed by the possibility bounds. As expected, it was verified that the width of the prediction intervals within the possibility bounds reduces as the possibility level α increases. More importantly, it was also observed that the observed hydrograph was enclosed by the 50% and 75% possibility bounds, except in a few cases. Increasing the possibility level to 90% reduces the range of predictions retained, at the cost of slightly increasing the fraction of the observations not enclosed, as observed in previous studies (Jacquin and Shamseldin, 2007, 2009).

Further research should explore the applicability of other criteria for evaluating model performance. At least some of these criteria should constrain the value of the internal variables of the model, in addition to glacier mass balance and snow cover, evaluating the likeliness of the simulated internal processes. This could help to further reduce predictive uncertainty and allow better enclosing the observed hydrographs, without significantly increasing the fraction of outliers.

Acknowledgements. This research was funded by FONDECYT, Research Project 11070130.

References

Amorocho, J. and Espildora, B.: Mathematical Simulation of the Snow Melting Processes, Water Science and Engineering Paper No. 3001, University of California, Davis, 1966.

Arnold, S., Attinger, S., Frank, K., and Hildebrandt, A.: Uncertainty in parameterisation and model structure affect simulation results in coupled ecohydrological models, Hydrol. Earth Syst. Sci., 13, 1789–1807, 2009, http://www.hydrol-earth-syst-sci.net/13/1789/2009/.

Arcadis Geotécnica: Ingeniería Conceptual Solución Ambiental ARD Proyecto Nueva Andina, CODELCO, Chile, 2007.

Bates, B. C. and Townley, L. R.: Nonlinear, discrete flood event models, 3, Analysis of prediction uncertainty, J. Hydrol., 99, 91–101, 1988.

HESSD

7, 2053–2084, 2010

Uncertainty analysis of a conceptual model of snowmelt runoff

A. P. Jacquin

Title Page

Abstract | Introduction

Conclusions | References

Tables | Figures

◀| |▶

◀ ▶

Back | Close

Full Screen / Esc

Printer-friendly Version

Interactive Discussion

Bárdossy, A., Mascellani, G., and Franchini, M.: Fuzzy unit hydrograph, Water Resour. Res., 42, W02401, doi:10.1029/2004WR003751, 2006.
Beven, K. J.: A manifesto for the equifinality thesis, J. Hydrol., 320, 18–36, 2006.
Beven, K. and Binley, A.: The future of distributed models: Model calibration and uncertainty prediction, Hydrol. Processes, 6, 279–298, 1992.
Beven, K. J. and Freer, J.: Equifinality, data assimilation, and uncertainty estimation in mechanistic modelling of complex environmental systems using the GLUE methodology, J. Hydrol., 249, 11–29, 2001.
Cheng, D. K.: Analysis of Linear Systems, Addison-Wesley Publishing Company, Reading, 1959.
Dou, C., Woldt, W., Dahab, M., and Bogardi, I.: Transient ground-water flow simulation using a fuzzy set approach, Ground Water, 35(2), 205–215, 1997.
Dubois, D. and Prade, H.: Fuzzy sets and probability: Misunderstandings, bridges and gaps, in: Proceedings 2nd IEEE International Conference on Fuzzy Systems, FUZZ-IEEE'93, San Francisco (California), 28 March–4 April 1993, 1059–1068, 1993.
Engeland, K., Xu, C.-Y., and Gottschalk, L.: Assessing uncertainties in a conceptual water balance model using Bayesian methodology, Hydrol. Sci. J., 50(1), 45–63, 2005.
Espíldora, B.: Instalación y operación de un laboratorio de hidrología de nieves, Seccion Hidrologia y Riego, Departamento de Obras Civiles, Universidad de Chile, Chile, 1968.
Ferson, S. and Ginzburg, L. R.: Different methods are needed to propagate ignorance and variability, Reliab. Eng. Syst. Safe., 54, 133–144, 1996.
Freissinet, C., Vauclin, M., and Erlich, M.: Comparison of first-order analysis and fuzzy set approach for the evaluation of imprecision in a pesticide groundwater pollution screening model, J. Contam. Hydrol., 37, 21–43, 1999.
Jacquin, A. P. and Shamseldin, A. Y.: Development of a possibilistic method for the evaluation of predictive uncertainty in rainfall-runoff modeling, Water Resour. Res., 43, W04425, doi:10.1029/2006WR005072, 2007.
Jacquin, A. P. and Shamseldin, A. Y.: Possibilistic uncertainty analysis of hydrological models, in: 8th International Conference on Hydroinformatics, Concepción, 12–16 January 2009, conf188a41, 2009.
Kamann, P. G.: Pronóstico estacional de deshielos en base a simulación, Memoria para Optar al Título de Ingeniero Civil, Universidad Técnica Federico Santa María, Chile, 1998.
Klir, G. J. and Folger, T. A.: Fuzzy sets, uncertainty and information, Prentice Hall, Singapore,

1992.
Kuckzera, G.: On the validity of first order prediction limits for conceptual hydrologic models, J. Hydrol., 103, 229–247, 1988.
Lei, J. H. and Schilling, W.: Preliminary uncertainty analysis-a prerequisite for assessing the predictive uncertainty of hydrologic models, Water Sci. Technol., 33(2), 79–90, 1996.
Misirli, F., Gupta, H. V., Sorooshian, S., and Thiemann, M.: Bayesian recursive estimation of parameter and output uncertainty for watershed models, in: Calibration of Watershed Models, edited by: Duan, Q., Gupta, H., Sorooshian, S., Rousseau, A., and Turcotte, R. V., American Geophysical Union, Washington, 113–124, 2003.
Matott, L. S., Babendreier, J. E., and Purucker, S. T.: Evaluating uncertainty in integrated environmental models: A review of concepts and tools, Water Resour. Res., 45, W06421, doi:10.1029/2008WR007301, 2009.
Montanari, A.: Large sample behaviors of the generalized likelihood uncertainty estimation (GLUE) in assessing the uncertainty of rainfall-runoff simulations, Water Resour. Res., 41, W08406, doi:10.1029/2004WR003826, 2005.
Montanari, A., Shoemaker, C. A., and van de Giesen, N.: Introduction to special section on Uncertainty Assessment in Surface and Subsurface Hydrology: An overview of issues and challenges, Water Resour. Res., 45, W00B00, doi:10.1029/2009WR008471, 2009.
Nash, J. E. and Sutcliffe, J. V.: River flow forecasting through conceptual models, Part I-A discussion of principles, J. Hydrol., 10, 282–290, 1970.
Özelkan, E. C. and Duckstein, L.: Fuzzy conceptual rainfall-runoff models, J. Hydrol., 253, 41–68, 2001.
Pappenberger, F. and Beven, K.: Ignorance is bliss: Or seven reasons not to use uncertainty analysis, Water Resour. Res., 42, W05302, doi:10.1029/2005WR004820, 2006.
Renard, B., Kavetski, D., Kuczera, G., Thyer, M. A., and Franks, S. W.: Understanding predictive uncertainty in hydrologic modeling: The challenge of identifying input and structural errors, Water Resour. Res., in press, doi:10.1029/2009WR008328, 2010.
Romanowicz, R., Beven, K., and Tawn, J. A.: Evaluation of predictive uncertainty in nonlinear hydrological models using a Bayesian approach, in: Statistics for the Environment 2: Water Related Issues, edited by: Barnett, V. and Feridun Turkman, K., John Wiley & Sons, Chichester, 297–317, 1994.
Rivera, A., Acuña, C., Casassa, G., and Bown, F.: Use of remotely sensed and field data to estimate the contribution of Chilean glaciers to eustatic sea-level rise, Ann. Glaciol., 34,

367–372, 2002.
Rojas, R., Batelaan, O., Feyen, L., and Dassargues, A.: Assessment of conceptual model uncertainty for the regional aquifer Pampa del Tamarugal – North Chile, Hydrol. Earth Syst. Sci., 14, 171–192, 2010, http://www.hydrol-earth-syst-sci.net/14/171/2010/.
Ross, T. J., Sellers, K. F., and Booker, J. M.: Considerations for using fuzzy set theory and probability theory, in: Fuzzy logic and probability applications: Building the gap, ASA-SIAM Series on Statistics and Applied Probability, edited by: Ross, T. J., Booker, J. M., and Parkinson, W. J., SIAM, Philadelphia, ASA, Alexandria, 87–104, 2002.
Seibert, J.: Estimation of Parameter Uncertainty in the HBV Model, Nord. Hydrol., 28(4/5), 247–262, 1997.
Thiemann, M., Trosset, M. Gupta, H., and Sorooshian, S.: Bayesian recursive parameter estimation for hydrologic models, Water Resour. Res., 37(10), 2521–2535, 2001.
Thorsen, M., Refsgaard, J. C., Hansen, S., Pebesma, E., Jensen, J. B., and Kleeschulte, S.: Assessment of uncertainty in simulation of nitrate leaching to aquifers at catchment scale, J. Hydrol., 242, 210–227, 2001.
Valdivia, P.: Inventario de glaciares Andes de Chile central (32°–35° Lat. S): Hoyas de los Ríos Aconcagua, Maipo, Cachapoal y Tinguiririca, in: Jornadas de Hidrología de Nieves y Hielos en América del Sur, PHI, UNESCO, Santiago, Chile, 3–8 December 1984, I6.1–I6.24, 1984.
Wagener, T., Wheater, H. S., and Gupta, H. V.: Identification and evaluation of watershed models, in: Calibration of Watershed Models, edited by: Duan, Q., Gupta, H. V., Sorooshian, S., Rousseau, A. N., and Turcotte, R., American Geophysical Union, Washington, 29–47, 2003.
Water Management Ltda.: Evaluación Recursos Hídricos Salar Punta Negra, Compañía Minera Escondida, Chile, 2001.
Yu, P.-S., Yang, T. C., and Chen, S. J.: Comparison of uncertainty analysis methods for a distributed rainfall-runoff model, J. Hydrol., 244, 43–59, 2001.
Zadeh, L. A.: Fuzzy sets as a basis for a theory of possibility, Fuzzy Sets and Systems, 1, 3–28, 1978.
Zadeh, L. A.: Possibility theory and soft data analysis, in: Mathematical Frontiers of the Social and Policy Sciences, edited by: Cob, B. L. and Thrall, R. M., Westview Press, Boulder (Colorado), 69–129, 1981.
Zadeh, L. A. and Desoer, C. A.: Linear System Theory: The State Space Approach, McGraw-

Hill, New York, London, 1963.
Zehe, E. and Blöschl, G.: Predictability of hydrologic response at the plot and catchment scales: The role of initial conditions, Water Resour. Res., 40, W10202, doi:10.1029/2003WR002869, 2004.
Zhang, K., Li, H., and Achari, G.: Fuzzy-stochastic characterization of site uncertainty and variability in groundwater flow and contaminant transport through a heterogeneous aquifer, J. Contam. Hydrol., 106, 73–82, 2009.
Zimmermann, H.-J.: Fuzzy Set Theory and Its Applications, Fourth Edition, Kluwer Academic Publishers, Boston, 2001.

HESSD
7, 2053–2084, 2010

Table 1. Fraction of observations not enclosed by the possibility bounds at selected possibility levels α, during the verification period.

Prior possibility distribution	Posterior possibility	α value 0%	75%	90%
π_{prior}	π_{post_1}	0.00	0.02	0.07
	$\pi_{post\_1,2}$	0.01	0.02	0.13
	$\pi_{post\_1,2,3}$	0.02	0.03	0.14
π_0	$\pi_{post\_0,1}$	0.01	0.02	0.10
	$\pi_{post\_0,1,2}$	0.01	0.02	0.11
	$\pi_{post\_0,1,2,3}$	0.01	0.04	0.15

HESSD

7, 2053–2084, 2010

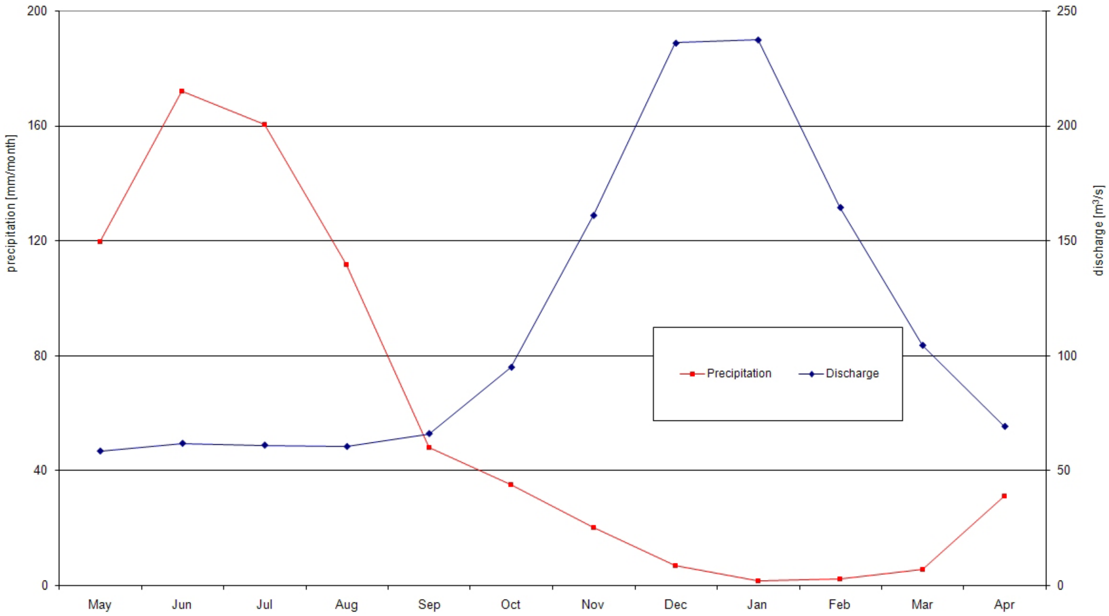

Fig. 1. Seasonal evolution of monthly precipitation and monthly mean discharge in Maipo at El Manzano catchment.

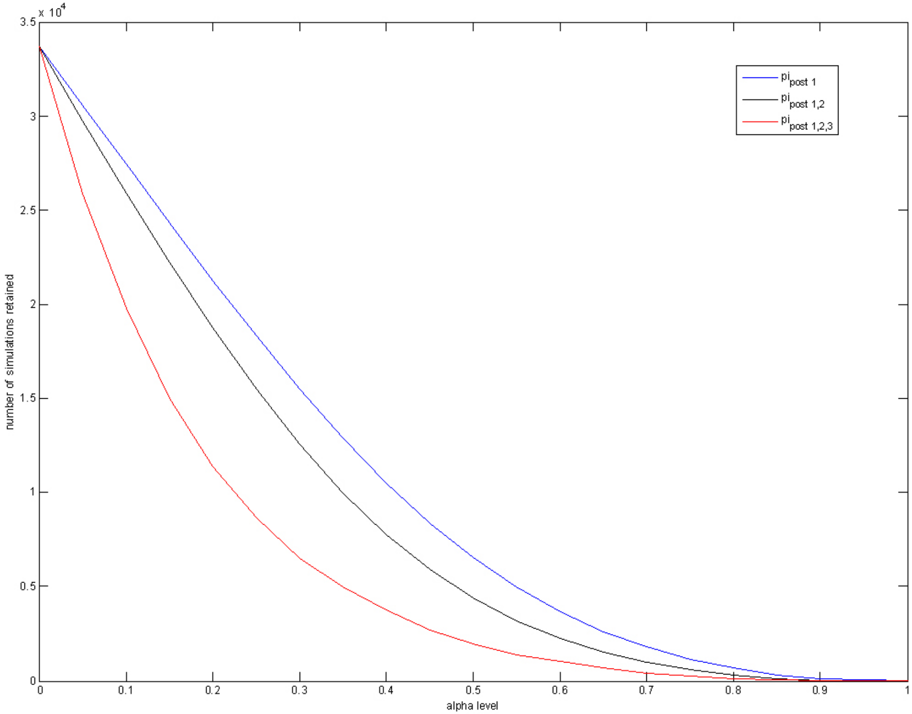

Fig. 2. Total number of simulations retained as a function of the possibility level α of the possibility distributions $\pi_{\mathrm{post\_1}}$, $\pi_{\mathrm{post\_1,2}}$ and $\pi_{\mathrm{post\_1,2,3}}$.

HESSD
7, 2053–2084, 2010

Uncertainty analysis of a conceptual model of snowmelt runoff

A. P. Jacquin

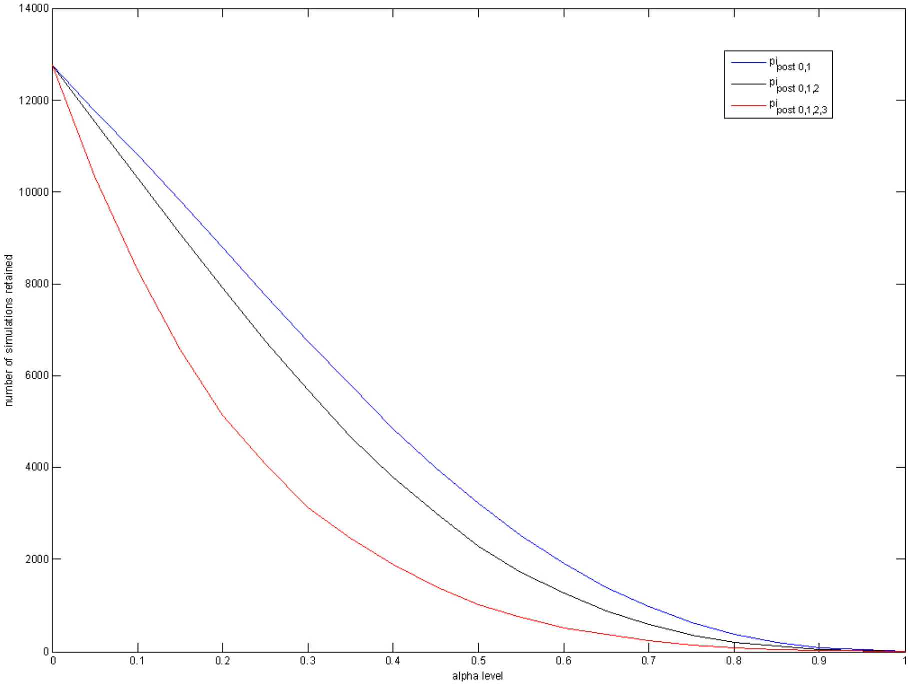

Fig. 3. Total number of simulations retained as a function of the possibility level α of the possibility distributions $\pi_{\text{post\_0,1}}$, $\pi_{\text{post\_0,1,2}}$ and $\pi_{\text{post\_0,1,2,3}}$.

HESSD

7, 2053–2084, 2010

Uncertainty analysis of a conceptual model of snowmelt runoff

A. P. Jacquin

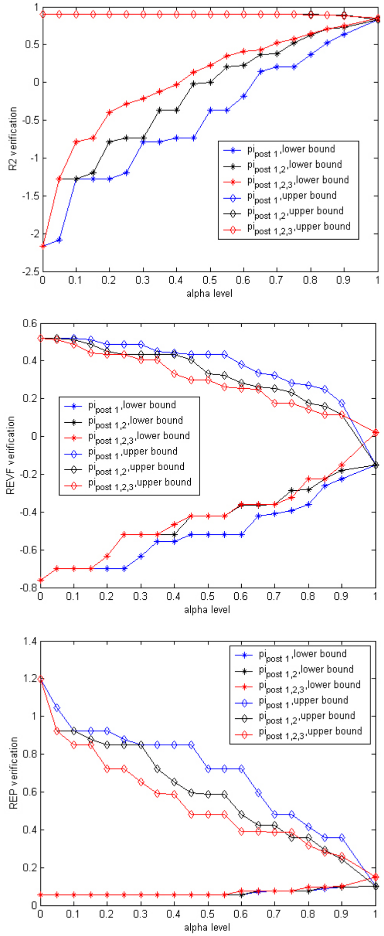

Fig. 4. Ranges of model performance statistics during the verification period of the simulations retained above given possibility levels α of the possibility distributions $\pi_{\text{post\_1}}$, $\pi_{\text{post\_1,2}}$ and $\pi_{\text{post\_1,2,3}}$.

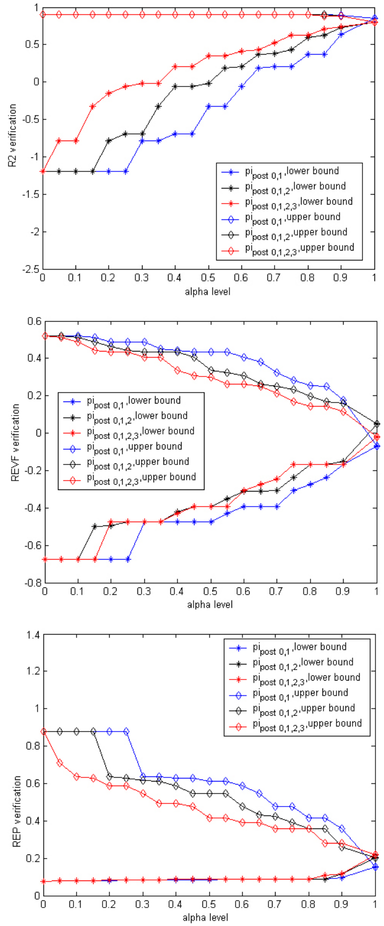

Fig. 5. Ranges of model performance statistics during the verification period of the simulations retained above given possibility levels α of the possibility distributions $\pi_{\text{post\_0,1}}$, $\pi_{\text{post\_0,1,2}}$ and $\pi_{\text{post\_0,1,2,3}}$.

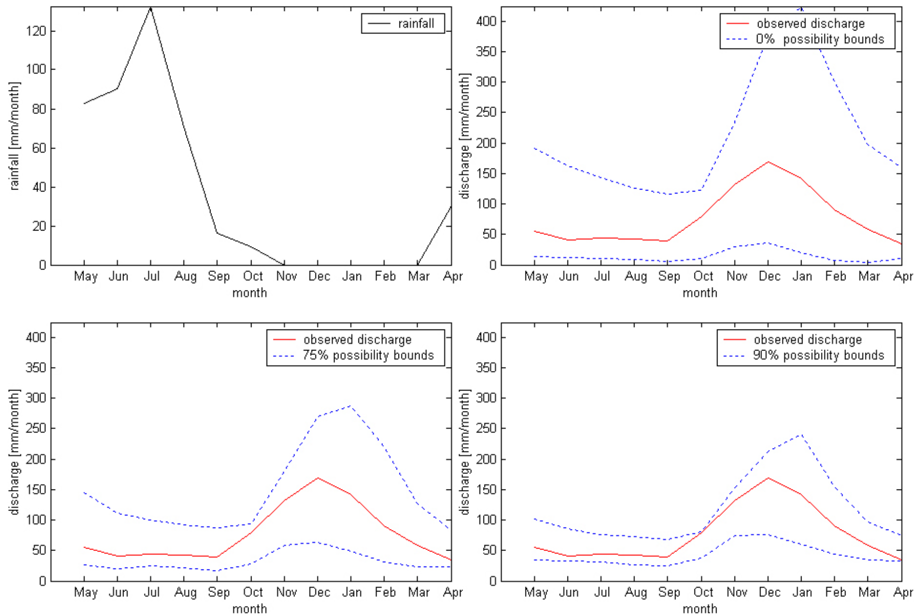

Fig. 6. Rainfall history, observed discharge and selected possibility bounds of discharge estimates during 1983/84, derived from the posterior possibility distribution π_{post_1}.

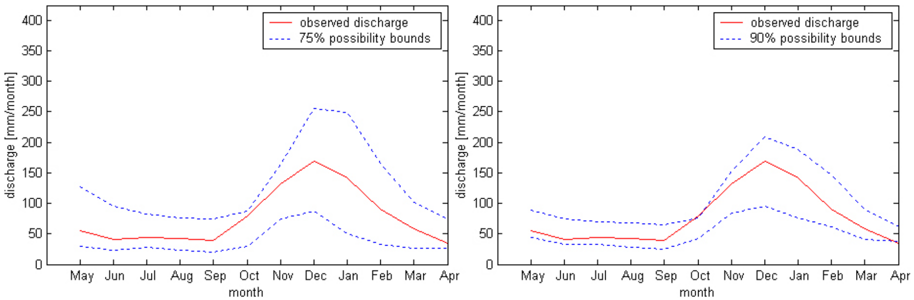

Fig. 7. Observed discharge and selected possibility bounds of discharge estimates during 1983/84, derived from the posterior possibility distribution $\pi_{post\_1,2,3}$.

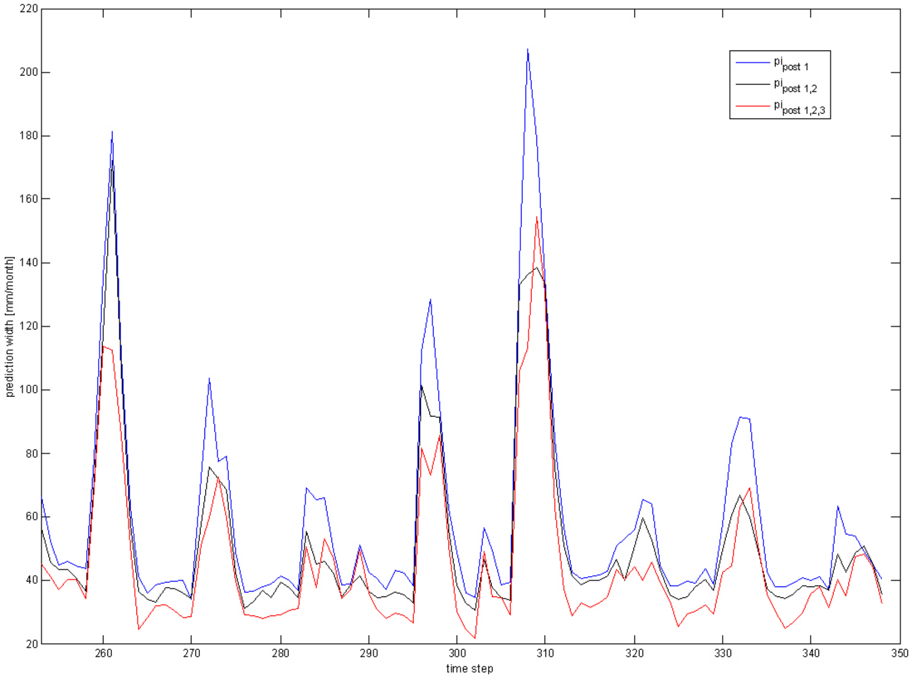

Fig. 8. Prediction width of the 90% possibility bounds derived from the possibility distributions $\pi_{\mathrm{post\_1}}$, $\pi_{\mathrm{post\_1,2}}$ and $\pi_{\mathrm{post\_1,2,3}}$, during the verification period.

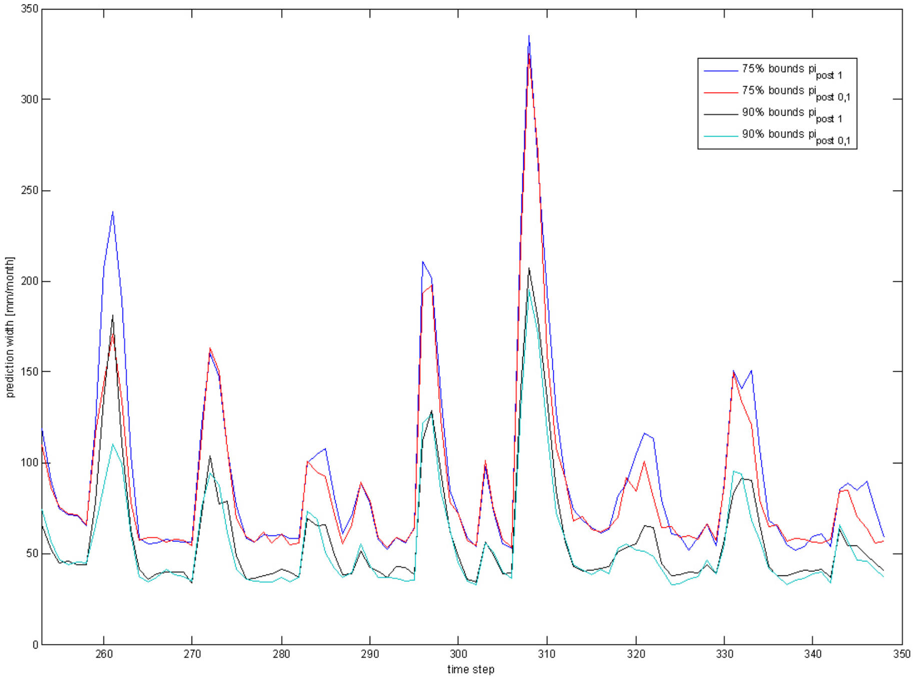

Fig. 9. Prediction width of the 75% and 90% possibility bounds derived from the possibility distributions $\pi_{\text{post\_1}}$ and $\pi_{\text{post\_0,1}}$, during the verification period.

HESSD
7, 2053–2084, 2010

Uncertainty analysis of a conceptual model of snowmelt runoff

A. P. Jacquin